Available online at www.sciencedirect.com
ScienceDirect
Solid State Communications 142 (2007) 110–113
solid state communications
www.elsevier.com/locate/ssc

Pulsed laser deposited nanostructured InN thin films as field emitters

K.P. Adhi[a,*], Sanjay Harchirkar[a], Suhas M. Jejurikar[a], P.M. Koinkar[a], M.A. More[a], D.S. Joag[a], L.M. Kukreja[b]

[a] *Centre for Advanced Studies in Materials Science and Solid State Physics, Advanced Materials Processing Laboratory, Department of Physics, University of Pune, Pune – 411 007, India*
[b] *Thin Film Laboratory, Raja Ramanna Centre for Advance Technology (RRCAT), Indore – 452 013, India*

Received 24 November 2006; accepted 29 December 2006 by H. Ohno
Available online 17 January 2007

Abstract

InN thin films were deposited on *c*-cut Al_2O_3 substrates using the DC plasma assisted pulsed laser deposition technique. X-ray diffraction (XRD) studies showed the single phase, polycrystalline nature of the InN thin films with wurtzite structure. Surface morphology of the films, as seen by atomic force microscopy (AFM), consisted of densely packed nanocrystalline grains of InN. The rms value of surface roughness was found to be ∼35 nm. AFM images also revealed the hexagonal features with sharp edges and protrusions of InN. The field emission characteristics of InN/Al_2O_3 were investigated in ultra high vacuum (1×10^{-8} Torr) using the diode configuration. The turn-on field, required to draw an emission current density of 10 μA/cm^2, was observed to be ∼3.5 V/μm. The maximum emission current density obtained was 230 μA/cm^2 when the applied electric field strength was ∼4 V/μm. The Fowler–Nordheim (FN) plot obtained from the current–voltage characteristic was found to be linear in accordance with the quantum mechanical tunneling phenomenon. The field enhancement factor, β, estimated from the slope of the FN plot was 21,167 cm^{-1}. To the best of our knowledge this is the first report of field emission studies of InN/Al_2O_3 with such high values of β, which is comparable to that obtained for GaN or IrO_2.

PACS: 81.15.Fg; 81.05.Ea; 68.55.Jk; 81.70.Fy; 61.10-i

Keywords: A. Thin films; A. Semiconductors; B. Laser processing; C. Field emission

1. Introduction

In the recent past, there has been growing interest in the area of field electron emission [1–3]. This interest stems from the fact that along with the scientific importance of enhancing basic understanding, it is also technologically essential in realizing various devices such as flat panel displays, electron sources in vacuum microelectronics etc. based on field emission. While new materials/compounds with better field emission properties are being explored [4–7], attempts are also being made to comprehend the influence of surface morphology, in terms of shape, structure viz. nano structures, nano-rods, pyramidal patterns etc., on field electron emission characteristics [8–11]. A variety of materials such as Gd_2O_3:Eu^{3+} [4], In_2O_3 [5], Si doped diamond like carbon films [6], GaN on molybdenum tips [7], carbon nano-tubes (CNT) [8] etc. have been studied for some time. It is only recently that wide band gap semiconductors such as ZnO nano-wires [9], AlN nano-rods [10], nanostructured GaN thin films [11] etc. have been the focus of field emission studies.

Among the wide band gap semiconductors, ZnO, AlN and GaN have stimulated extensive research interest due to their potential applications as field emitters. InN, however, is yet to be examined to that extent, which is probably due to its low dissociation temperature, making the synthesis of InN very difficult. InN is unstable above 550 °C. However, in the last few years, the interest in InN has been on the rise, both for fundamental understanding as well as its potential applications [12,13]. From the point of view of basic studies, some of the issues being addressed are (a) accuracy and variation in the determination of band gap of InN. Earlier the

* Corresponding author. Tel.: +91 20 2569 2678; fax: +91 20 2569 1684.
E-mail address: kpa@physics.unipune.ernet.in (K.P. Adhi).

0038-1098/$ - see front matter © 2007 Elsevier Ltd. All rights reserved.
doi:10.1016/j.ssc.2006.12.027

value obtained was 1.89 eV [13,14] but recent studies suggest the band gap to vary between 0.7 and 0.9 eV [15]. Several mechanisms such as the oxygen contamination, quantum size effects, Mie resonance and the Burstein–Moss effects have been used to explain the deviation in case of InN thin films, and (b) the lattice parameters of wurtzite InN, reported in the literature are observed to be different leading to uncertainty [16]. In terms of practical use, InN and its alloys with GaN and AlN make it possible to extend the emission range of nitrides from the ultraviolet to near infra-red region [17]. Recent study reveals that InN has promising transport and optical properties and a large drift velocity at room temperature even higher than that of GaN. Hence, InN has a high potential as a material for the fabrication of high-speed, high-performance heterojunction FETs [17] etc.

Study of InN as a field emitter has not yet received significant attention. To the best of our knowledge, there are only a couple of reports of InN nano-rods/structures as field emitters [18,19]. Here we report a systematic study of field emission characteristics from pulsed laser deposited polycrystalline InN thin films on *c*-axis oriented Al_2O_3.

2. Experimentation

Radiation from an excimer laser (gas KrF, wavelength $\lambda = 248$ nm, pulse duration $t_p = 20$ ns, repetition rate = 5 Hz) was focused on an indium target (purity 99.99%) mounted in the deposition chamber. The polar angle between the incident radiation and the normal to the target surface was 45°. The fluence incident on the targets surface was 0.5 J/cm^2. Prior to deposition, the *c*-cut Al_2O_3 substrates were ultrasonically degreased, sequentially, in trichloroethylene, acetone and methanol for five minutes each and dried under a nitrogen jet. The cleaned substrate was mounted on a heater and placed parallel to the target at a distance of 5 cm in the deposition chamber. A copper ring was mounted in between the indium target and the Al_2O_3 substrate at a distance of 0.5 cm from the target surface. The chamber was evacuated to a base vacuum of 1×10^{-5} Torr. High purity (99.999%) nitrogen was introduced into the chamber and maintained at a pressure of 25 mTorr throughout the deposition process. Before starting the deposition, nitrogen plasma was initiated by applying 900 V (DC) to the copper ring with respect to the indium target. Fundamental to the DC plasma assisted PLD process is the generation of reactive nitrogen species, which reacts with the indium plasma plume to form InN. The reacted species impinge, inelastically, onto the substrate, which was maintained at 500 °C throughout the deposition. During deposition the target was continuously rotated at 10 rpm to avoid texturing/pitting of the target surface. After the deposition, the samples were slowly cooled to room temperature in nitrogen ambient at atmospheric pressure.

The thickness of the deposited thin films was measured using a Tally step instrument at four or five different positions on the films. X-ray diffraction (XRD) was used to study the phase formation, crystallographic orientation and structural quality of the deposited thin films. The Cu Kα radiation at wavelength of 1.542 Å was used for the diffraction studies. The surface morphology of the sample was investigated using atomic force microscopy (AFM-Jeol, JSPM 5200) in contact mode. The field emission studies were carried out in an ultra high vacuum chamber evacuated to a base vacuum of 1×10^{-8} Torr. A typical 'diode' configuration, consisting of a phosphor coated tin-oxide glass plate anode (circular disk of diameter 50 mm) and the deposited thin film cathode was used. The sample was mounted on a stainless steel stub connected to a linear motion drive, which helps in adjusting the distance between the anode and the cathode. In the present study, the distance between the two was adjusted to 5 mm. The details of the field emission set up are mentioned elsewhere [11].

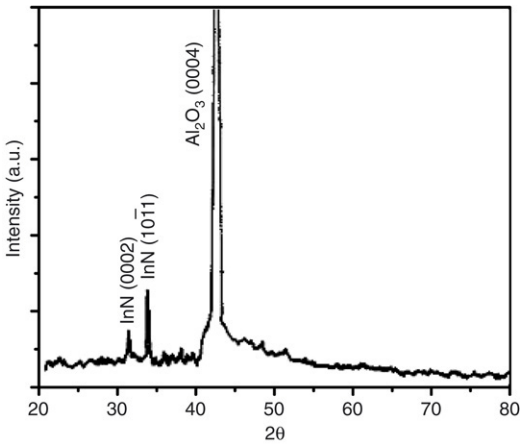

Fig. 1. X-ray diffractogram of polycrystalline InN thin films deposited on *c*-axis Al_2O_3.

3. Results and discussions

The thin films deposited on *c*-cut Al_2O_3 had uniform thickness of 400 ± 10 nm.

Fig. 1 shows the XRD (θ–2θ) pattern of the deposited thin film on the *c*-axis oriented Al_2O_3 substrate. The peaks located at 2θ values of 31.4° and 33.2° correspond to wurtzite InN (0002) and (10$\bar{1}$1) planes respectively, indicating the polycrystalline nature of the thin films. The third peak located at $2\theta = 42°$ corresponds to the (0004) plane of the Al_2O_3 substrate. Hence, the single-phase, polycrystalline InN thin films with wurtzite structure were successfully deposited on *c*-axis oriented Al_2O_3 substrates.

The surface morphology of the InN thin film is as shown in Fig. 2(a) and (b). The following observations can be made from Fig. 2(a); (i) the surface morphology of the deposited film shows densely packed, elongated nanocrystalline grains of InN (ii) the surface of the thin film is rough i.e. the variation in height (rms surface roughness) across the grains over the complete film is estimated to be ∼3.5 nm. Similar results were obtained from different regions of the InN thin films suggesting uniformity in the deposition and growth process. Fig. 2(b) shows the 3D image of the InN thin film of the same region as shown in Fig. 2(a). It is observed that (i) the elongated grains, seen in Fig. 2(a), actually show multiple hexagonal structures with sharp edges and protrusions and (ii) each grain shows a rough surface. The multiple hexagonal structures with sharp edges and protrusions are uniformly distributed over the entire

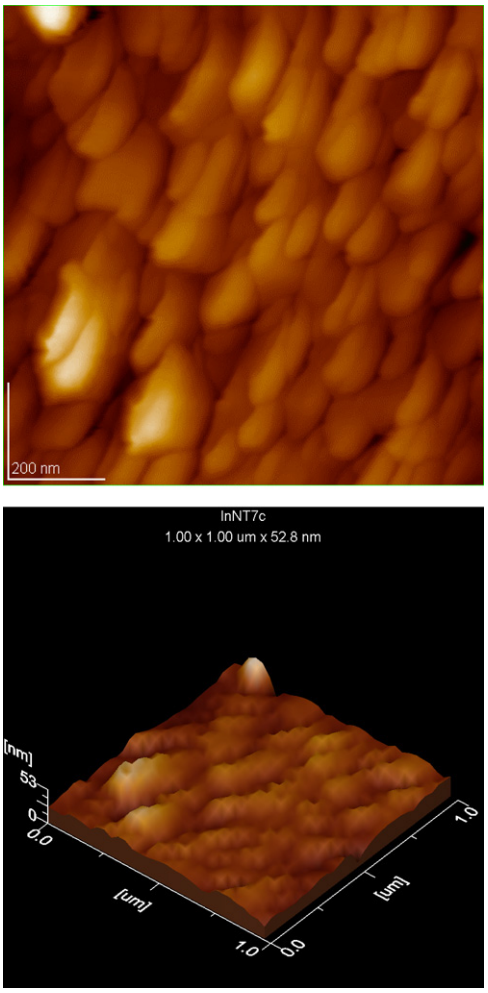

Fig. 2. AFM images of InN thin films deposited on c-axis Al_2O_3 showing the surface morphology in (a) two dimensions and (b) three dimensions—The sharp edges of the hexagonal structures of InN thin films are clearly visible.

surface and are observed to be of the order of a few 10's of nanometers.

The field emission pattern consisted of bright spots with very stable intensity. Fig. 3 shows the plot of measured field emission current density (J) as a function of applied electric field strength (E) for the polycrystalline InN thin films deposited on c-cut Al_2O_3. An emission current density of ~5.0 μA/cm^2 was drawn for an applied electric field strength of ~1.5 V/μm reproducibly. The current density was observed to double (10 μA/cm^2) on enhancing the applied electric field from 1.5 to ~3.5 V/μm. The turn on field (E_{to}) is defined as the applied electric field required drawing a current density of 10 μA/cm^2, which is needed for typical operation of flat panel displays [10]. Hence, in the case of InN thin films deposited on c-axis Al_2O_3, E_{to} is 3.5 V/μm, which is comparable with that of carbon nanotubes [8], AlN nano-needle arrays [20], and a-GaN films [11]. With further increase in the field strength, the emission current density is observed to increase exponentially and a maximum current density of ~230 μA/cm^2 was obtained for an applied electric field strength of 4 V/μm. The reason for the low turn on field and high field emission current density

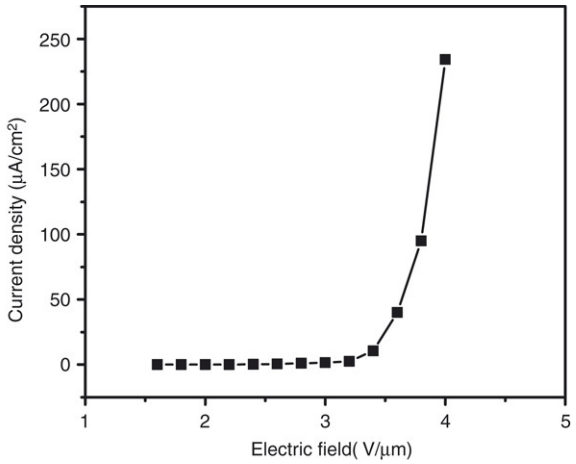

Fig. 3. Plot of emission current density, J (μA/cm^2) as a function of applied electric field E, (V/μm).

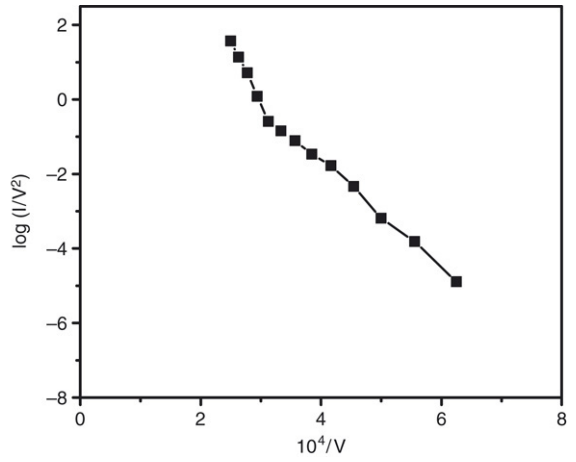

Fig. 4. F–N plot of log (I/V^2) versus $(10^4/V)$.

is probably due to the nanometric features of the hexagonal structures of InN thin films, observed in Fig. 2(b).

The field emission current density–electric field (J–E) characteristics were analyzed using the Fowler–Nordheim (FN) equation.

$$J = (A\beta^2 E^2/\phi)\exp(-B\phi^{3/2}/\beta E),$$

where ϕ is the work function of InN, β is the field enhancement factor, A and B are the constants having values 1.56×10^{-10} (A V^{-2} eV) and 6.83×10^3 (V eV$^{-3/2}$ μm^{-1}), respectively. Fig. 4 shows the FN plot of log (I/V^2) as a function of $10^4/V$. Within the measurement range, the plot shows a linear relationship, which follows the quantum mechanical tunneling process.

Field enhancement factor β is associated with the magnitude of the local electric field existing at the emission sites in the InN thin films and is defined as,

$$E_{local} = \beta E = \beta \frac{V}{d}$$

where E_{local} is the local electric field close to the emission sites, d is the average distance between the electrodes and V is the applied voltage. The field enhancement factor β is

estimated from the slope 'm' of the FN plot, using the relation $\beta = [-2.97 \times 10^3 \times \Phi^{3/2}]/m$, provided Φ, the work function of InN is known. Shih et al. report the work function of InN, Φ to be 5.1 eV [19]. To the best of our knowledge, this is the only report on the work function Φ in the literature. Due to non-availability of the actual value, Ji et al. [18] in their work had assumed Φ for InN to be 1 eV. They, however, are of the opinion that Φ should have a value similar to other nitrides. The field enhancement factor β, in our case, is calculated to be 21,167 cm^{-1}. The high value of β obtained for InN is comparable to that of GaN [21] and IrO_2 [22]. These excellent field emission characteristics, viz low turn on voltage, drastic enhancement in emission current density for small variation in applied field and high field enhancement factor β demonstrate the strong possibility of use of InN/Al_2O_3 as field emitters in device applications.

4. Conclusion

Polycrystalline InN thin films, as confirmed from XRD analysis, were successfully deposited on c-cut Al_2O_3 substrates using the pulsed laser deposition technique. AFM images revealed a rough surface with sharp edges and protrusions of nanometer dimensions, which help in obtaining field electron emission at low applied electric field. The field emission studies of indium nitride thin films show low turn on field, which is about 3.5 V/μm, and the corresponding current density is ∼10 μA/cm^2. The maximum current density of ∼230 μA/cm^2 was observed at an applied electric field of 4.0 V/μm. The field enhancement factor β is estimated to be 21,167 cm^{-1}. The above results indicate strongly that InN nanostructured thin films can be used successfully in integrated field emitting devices.

Acknowledgement

The authors, KPA, LMK and SMJ, thank DAE-BRNS for the financial support extended for carrying out this work under the project sanction No. (2002/34/21/BRNS).

References

[1] F.C.K. Au, K.W. Wong, Y.H. Tang, Y.F. Zhang, I. Bello, S.T. Lee, Appl. Phys. Lett. 75 (1999) 1700.
[2] H.-M. Kim, T.W. Kang, K.S. Chung, J.P. Hong, W.B. Choi, Chem. Phys. Lett. 377 (2003) 491.
[3] I. Berishev, A. Bensaoula, I. Rusakova, A. Karabutov, M. Ugarov, P. Ageev, Appl. Phys. Lett. 73 (1998) 1808.
[4] Kuo-Min Lin, Yuan-Yao Li, Nanotechnology 17 (2006) 4048.
[5] S. Kar, S. Chakrabarti, S. Chaudhuri, Nanotechnology 17 (2006) 3058.
[6] A.A. Evtukh, V.G. Litovchenko, Y.M. Litvin, D.V. Fedin, O.S. Dzyan, Yu.N. Pedchenko, A.G. Chakhovskoi, T.E. Felter, J. Vac. Sci. Technol. B 21 (2003) 627.
[7] S. Hasegawa, S. Nishida, T. Yamashita, H. Asahi, Thin Solid Films 487 (2005) 260.
[8] J. Robertson, W.I. Milne, K.B.K. Teo, M. Chhowalla, AIP Conf. Proc. 633 (2002) 537.
[9] S.H. Jo, J.Y. Lao, Z.F. Ren, R.A. Farrer, T. Baldacchini, J.T. Fourkas, Appl. Phys. Lett. 83 (2003) 4821.
[10] Y.B. Tang, H.T. Cong, Z.G. Zhao, H.M. Cheng, Appl. Phys. Lett. 86 (2005) 153104.
[11] D.S. Joag, D.J. Late, U.D. Lanke, Solid State Commun. 130 (2004) 305.
[12] E. Bellotti, B.K. Doshi, K.F. Brennan, J.D. Albrecht, P.P. Ruden, J. Appl. Phys. 85 (1999) 916.
[13] S.K. O'Leary, B.E. Foutz, M.S. Shur, U.V. Bhapkar, L.F. Eastman, J. Appl. Phys. 83 (1998) 826.
[14] T.L. Tansley, C.P. Foley, J. Appl. Phys. 59 (1986) 3241.
[15] A.G. Bhuiyan, A. Hashimoto, A. Yamamoto, J. Appl. Phys. 93 (2003) 2779 and references therein.
[16] M.F. Wu, S.Q. Zhou, A. Vantomme, Y. Huang, H. Wang, H. Yang, J. Vac. Sci. Technol. A 24 (2006) 275.
[17] A.G. Bhuiyan, A. Hashimoto, A. Yamamoto, J. Appl. Phys. 94 (2003) 2779.
[18] X.H. Ji, S.P. Lau, H.Y. Yang, S.F. Yu, Nanotechnology 16 (2005) 3069.
[19] C.F. Shih, N.C. Chen, P.H. Chang, K.S. Liu, J. Cryst. Growth 281 (2005) 328.
[20] Q. Zhao, J. Xu, X.Y. Xu, Z. Wang, D.P. Yu, Appl. Phys. Lett. 85 (2004) 5331.
[21] S.M. Jejurikar, P.M. Koinkar, M.A. More, D.S. Joag, K.P. Adhi, L.M. Kukreja, Communicated.
[22] R.-S. Chen, Y.-S. Huang, Y.-M. Liang, C.-S. Hsieh, D.-S. Tsai, K.-K. Tiong, Appl. Phys. Lett. 84 (2004) 1552.